

Strain dependence of defect-induced tunneling states in $\text{KCl}:\text{Li}^+$

R. P. Devaty and A. J. Sievers

Laboratory of Atomic and Solid State Physics, and Materials Science Center, Cornell University, Ithaca, New York 14853

(Received 21 August 1978)

The far-infrared absorption data of Kahan *et al.* on the pressure dependence of impurity-induced lattice modes in $\text{KCl}:\text{Li}^+$ are analyzed in terms of a static three-dimensional potential that separates into a sum of three one-dimensional symmetric double-minimum potentials. Numerical calculations have been performed on two model potentials, a quartic well with a quadratic barrier (two parameters) and a harmonic well perturbed by a Gaussian barrier (three parameters). We show that both potentials can account for the strain dependence of the observed absorption lines and the ^6Li - ^7Li isotope effect for the lowest frequency line. In each case the potential-barrier height is found to depend linearly on the lattice constant, while the off-center displacement (coordinate of minimum energy) is weakly linear in strain up to an abrupt collapse at the lattice constant for which the barrier disappears. The strain dependence of $\text{KCl}:\text{Li}^+$ can be partitioned into three regimes of behavior: an off-center (tunneling) region, a very anharmonic transition region, and a harmonic region perturbed by an increasingly weak anharmonicity.

I. INTRODUCTION

Pressure, when coupled with far-infrared spectroscopy, should be an important probe of the local defect potential of impurities which induce low-frequency modes in alkali halides. Among the most studied host-lattice-impurity systems are $\text{KBr}:\text{Li}^+$ and $\text{KCl}:\text{Li}^+$. The on-center nature of a Li^+ substitutional impurity in KBr and its off-center behavior in $\text{KCl}:\text{Li}^+$ were determined by a variety of experimental techniques.¹ Nolt and Sievers² investigated the dependence of the frequency shift of defect modes in $\text{KBr}:\text{Li}^+$ on uniaxial stress. They found by symmetry arguments that the impurity occupies the normal lattice site of the cation it replaces. This result was in disagreement with theoretical predictions of off-center behavior,^{3,4} which led to a better understanding of the defect potential.⁵ Recently, Kahan *et al.*⁶ varied the hydrostatic pressure and measured far-ir properties of several host-lattice-impurity combinations. They observed a transition from off-center to on-center behavior in $\text{KCl}:\text{Li}^+$ with increasing pressure, verifying a prediction by Quigley and Das.⁵ This result was the first spectroscopic evidence suggesting a connection between off-center and on-center defect systems. Furthermore, Kahan *et al.*⁶ established a correspondence between the properties of highly stressed $\text{KCl}:\text{Li}^+$ ($-dr/r = 0.65\%$, r is the lattice constant) and unstressed $\text{KBr}:\text{Li}^+$.

Extremely anharmonic potentials are required to model the behavior of these low-frequency impurity-activated modes. The most common approximation used to study off-center systems is the tunneling model developed by Gomez, Bowen, and Krumhansl⁷ (GBK). A basis of pocket states

(typically harmonic-oscillator eigenfunctions) localized at each of the equivalent off-center sites of minimum potential energy is chosen. Usually, only the ground-state wave function of each pocket potential is used. Mixing with excited-state multiplets is ignored. A matrix taking overlap and external fields into account is constructed in this basis and diagonalized to determine the splittings and eigenfunctions of the lowest-energy manifold of states. This procedure is valid only when the energy barriers between pockets exceed the energy levels and splittings under consideration. Excited-state multiplets may be treated in a similar manner if they lie sufficiently below the barrier maximum. The GBK model cannot be used to fit the strain dependence of the far-ir absorption lines in $\text{KCl}:\text{Li}^+$ because the assumptions about barrier height are violated, especially at high strains for which the Li^+ ion is driven on-center.

Kahan *et al.*⁶ interpreted their data in terms of a three-dimensional generalization of a one-dimensional symmetric double-square-well potential. Three parameters—barrier height, barrier width, and total well width—were required to obtain fits for the defect-mode frequencies. The large isotope effect observed for the lowest frequency or tunneling mode in $\text{KCl}:\text{Li}^+$ was explained qualitatively in this model. However, almost no correlation was found between the values of the three parameters at one strain and the next. Consequently, little insight was gained from the form of the potential at each strain. The model was too crude to give meaningful information on details of the local defect potential such as the variation of the barrier height with strain.

This paper reports calculations on two symmetric double-minimum potentials of the type used

by Kahan *et al.*,⁶ but more realistic in terms of shape and smoothness: a quartic plus harmonic (QH) potential,

$$v(x) = v_4 x^4 + v_2 x^2 \quad (1)$$

and a harmonic potential perturbed by a Gaussian barrier (GB),

$$v(x) = Ax^2 + B \exp(-Cx^2). \quad (2)$$

By fitting these models to the data and comparing the results we can make some empirical statements about the form of the defect potential and the dependence of its parameters upon strain. A potential such as Eq. (1) can be regarded as a "spin Hamiltonian" approximation or truncated expansion of either the true defect potential or the potential resulting from a first-principles calculation of the type performed by Quigley and Das.⁵

The environment of an impurity in an alkali halide is not static due to the effects of the defect-lattice interaction. Hence, it is best to interpret the variable x not as a position in real space, but as a generalized coordinate. This choice is in the spirit of our goal, which is to account for the resultant frequencies observed experimentally, including all dynamical effects.

Section II begins with a discussion of the symmetry properties of the model. Transitions are assigned to experimental absorption lines and our choices of potential $v(x)$ are motivated. Also, the computational methods used to calculate eigenvalues and fit them to the data are summarized.

In Sec. III, results of calculations with each potential are presented and interpreted. Both model potentials are able to account for most of the features in the strain-dependent absorption spectra and the tunneling mode (ground-state multiplet) isotope effect, but the QH potential does the job with one less parameter. The strain dependence of the parameters is found to be continuous. These results allow us to identify three regimes of behavior in the data. Finally, some comparison of our potentials with the results of calculations by Quigley and Das⁵ is made.

II. THE MODELS

A. Symmetry properties

A potential intended to model the accepted picture of off-center behavior in $\text{KCl}:\text{Li}^+$ must possess a minimum in each of the eight $[111]$ directions. The most mathematically tractable potential of this type is a sum of three one-dimensional potentials,

$$V(x, y, z) = v(x) + v(y) + v(z), \quad (3)$$

where $v(x)$ is a symmetric double well with minima

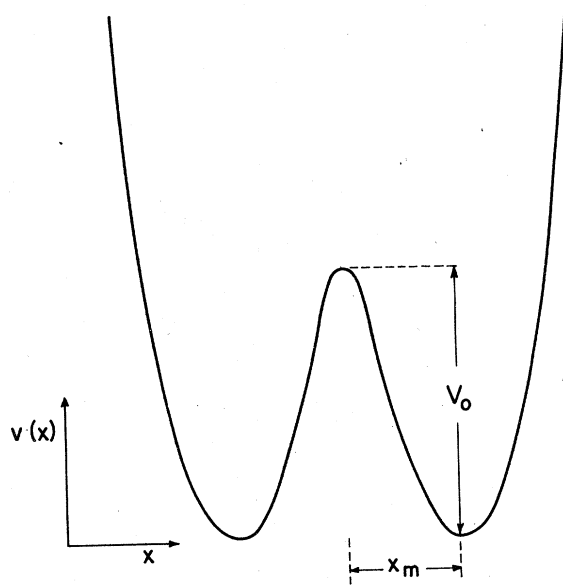


FIG. 1. One-dimensional double-minimum potential showing barrier height V_0 and off-center displacement of minimum potential energy x_m .

at $\pm x_m$ (see Fig. 1). To reduce the number of parameters we assume that the one-dimensional functions are identical. If V_0 is the barrier for tunneling between adjacent wells, a consequence of this form is that the barrier for tunneling across a body diagonal and along a diagonal of a face of the cube formed by the eight minima are $3V_0$ and $2V_0$, respectively. Before we have even chosen a function $v(x)$, we find that $V(x, y, z)$ is quite restricted. Of course, none of these constraints are strictly valid for Li^+ in KCl , and we shall note some of the consequences later.

The form (3) was chosen so that the stationary Schrödinger equation

$$H\Psi(x, y, z) = (T + V)\Psi = E\Psi \quad (4)$$

separates into three identical single variable eigenvalue problems that are relatively straightforward to solve. Suppose the solutions to the one-dimensional problem are, in ascending order, the energies $e_0, e_1, e_2, e_3, \dots$ with associated eigenfunctions $\varphi_0(x), \varphi_1(x), \varphi_2(x), \varphi_3(x), \dots$. The eigenfunctions possess definite parity and form a complete orthonormal set. The functions with even indices have even parity; the rest are odd. The eigenfunctions of the 3D problem are sums of product states of 1D eigenfunctions, and the energies are sums of the corresponding eigenvalues. For example, the ground-state energy is

$$E_0 = e_0 + e_0 + e_0 = 3e_0 \quad (5)$$

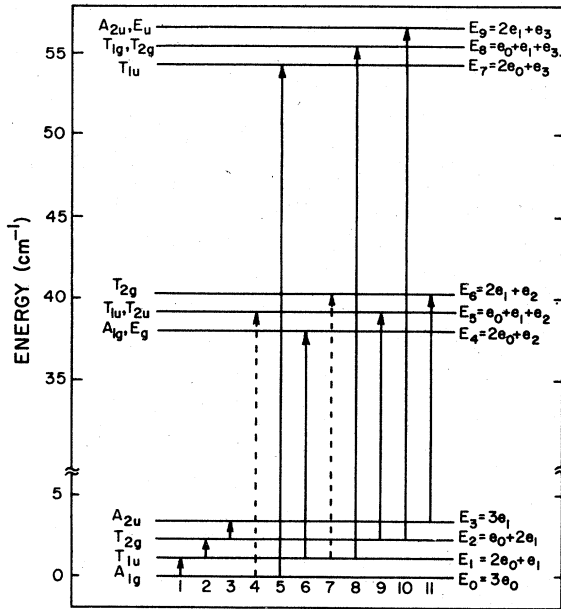


FIG. 2. Lowest-energy levels for the potential $V(x, y, z) = v(x) + v(y) + v(z)$ drawn to approximate the situation in KCl:Li⁺ at zero applied pressure. $v(x)$ has a large barrier so that the tunneling splitting is small and the levels are arranged in three distinct multiplets. The allowed electric dipole transitions from the ground state multiplet are shown. The transitions marked with dotted lines are electric dipole forbidden in the model, but are discussed in the text. The levels are labeled with the appropriate irreducible representations of O_h on the left and the sum of energies from the 1D potential $v(x)$ on the right.

and the wave function is

$$\Psi(x, y, z) = \varphi_0(x)\varphi_0(y)\varphi_0(z). \quad (6)$$

The state is nondegenerate since there exists only one combination of 1D eigenfunctions with energy E_0 . The first excited state is triply degenerate because there are three linearly independent combinations of product states with eigenvalue

$$E_1 = 2e_0 + e_1. \quad (7)$$

The entire spectrum of H can be constructed in this manner.

A potential of the form given by Eq. (3) has octahedral symmetry, so the eigenfunctions must transform according to the irreducible representations of the group O_h . Figure 2 is an energy-level diagram depicting the lowest three multiplets of states labeled with the irreducible representations of O_h . The figure is drawn for a high-barrier potential such that the tunneling splitting, $e_1 - e_0$, is much less than $e_2 - e_0$ and $e_3 - e_0$. Figure 2 also displays the allowed electric dipole transitions from the lowest energy, or "tunneling," multiplet. There are a total of 13 transitions allowed

by cubic symmetry within the ground-state multiplet and from this multiplet to the lowest excited-state multiplets, but the fact that our cubic potential is separable reduces the number of electric-dipole-allowed transitions to the nine indicated by solid lines. The remaining four transitions⁸ connect states for which two of the three 1D eigenfunctions differ, so the matrix elements vanish by orthogonality of the pairs of 1D eigenfunctions not connected by the dipole operator. The transitions indicated by dotted lines are two of these forbidden transitions, but they closely match an observed absorption line. No line corresponds to the remaining forbidden frequency ($E_8 - E_3$ and $E_7 - E_2$).

The 11 frequencies shown in Fig. 2 are not unique, but satisfy the following conditions:

$$\begin{aligned} \omega_1 &= \omega_2 = \omega_3 = e_1 - e_0, \\ \omega_6 &= \omega_9 = \omega_{11} = e_2 - e_1, \\ \omega_5 &= \omega_8 = \omega_{10} = e_3 - e_0, \\ \omega_4 &= \omega_7 = e_1 + e_2 - 2e_0. \end{aligned} \quad (8)$$

An additional condition is

$$\omega_4 = \omega_6 + 2\omega_1. \quad (9)$$

Thus only three distinct frequencies exist for the allowed transitions involving the tunneling multiplet and the first two excited-state multiplets. We consider transitions from all states in the tunneling multiplet because at low pressures the level spacings are sufficiently small (0.82 cm⁻¹ for KCl:⁷Li⁺ and 1.15 cm⁻¹ for KCl:⁶Li⁺ at zero strain⁹) that even at liquid-helium temperatures all four levels are populated. The relative populations for ⁶Li⁺ impurities in unstrained KCl at 4.2 °K are E_0 , 21%; E_1 , 43%; E_2 , 29%; and E_3 , 7%. As the hydrostatic pressure is increased, the tunneling splitting increases and the higher tunneling levels are depopulated.

B. Assignment of transitions and choice of $v(x)$

To assign model transitions to experimental absorption lines, we examine some far-ir absorption spectra. Figure 3(a) is a reproduction from the paper by Kirby *et al.*¹⁰ showing the 40-cm⁻¹ excited-state absorption band of KCl:⁶Li⁺ at zero strain for two temperatures. The strong tunneling line at 1.15 cm⁻¹, which does not appear in the figure, is assigned to ω_1 , ω_2 , and ω_3 . There are at least two peaks in the spectrum—near 37 and 50 cm⁻¹. The 37-cm⁻¹ peak becomes stronger when the temperature is increased, whereas the 50-cm⁻¹ peak does not change. Since the transitions

$$\omega_6 = \omega_9 = \omega_{11} \quad (10)$$

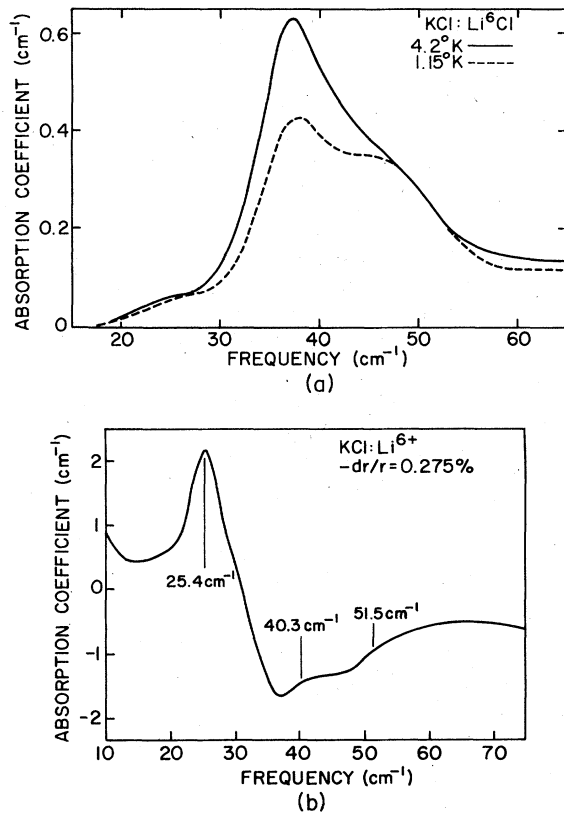


FIG. 3. (a) Temperature dependence of the $\text{KCl}:\text{Li}^{6+}$ 40- cm^{-1} absorption band. The transitions ω_6 and ω_5 are assigned to the lines at 37 and 50 cm^{-1} , respectively. (b) $\text{KCl}:\text{Li}^{6+}$ absorption spectrum for a high-concentration sample at 0.275% strain. The peaks are assigned, in ascending order, to the frequencies ω_6 , ω_4 , and ω_5 .

do not originate from the ground state, the absorption strength at this frequency will increase with temperature as the upper three levels of the tunneling multiplet become populated. Therefore, we assign the 37- cm^{-1} line to ω_6 . Since one of the transitions

$$\omega_5 = \omega_8 = \omega_{10} \quad (11)$$

originates from the ground state, there will be little change in the absorption when the temperature decreases from 4.2 to 1.15 $^{\circ}\text{K}$. Thus we assign the 50- cm^{-1} line to ω_5 . Note that

$$\omega_5 > \omega_6 \quad (12)$$

in agreement with the data.

Figure 3(b), taken from Kahan *et al.*,⁶ shows a spectrum measured at the strain $-dr/r = 0.275\%$. The tunneling line (transitions within the ground-state multiplet), found at 6 cm^{-1} for this strain, is not shown. We observe three lines associated with transitions from the ground-state multiplet to excited-state multiplets. The lines at 25.4 and

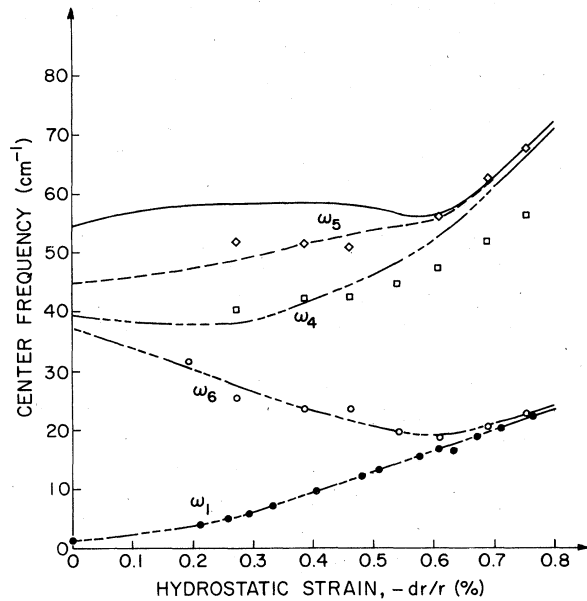


FIG. 4. Strain dependence of $\text{KCl}:\text{Li}^{6+}$ absorption frequencies. Symbols indicate data from Kahan *et al.*; solid lines and dashed lines represent the best fits obtained with the QH and GB potentials, respectively. Identical fits (alternating dashes and lines) were obtained for the lowest three transitions: ω_1 , ω_6 , ω_4 .

51.4 cm^{-1} match the frequencies ω_6 and ω_5 , respectively (see Fig. 4). Following Kahan *et al.*,⁶ the weak line at 40.3 cm^{-1} , although electric dipole forbidden in our model, is assigned to ω_4 . Evidently this transition is allowed for the true defect potential.

Although not shown in Fig. 4, two tunneling frequencies appear in Kahan's data over a wide range of strains. Hetzler and Walton¹¹ also observed unequal tunneling splittings at zero strain using phonon spectroscopy. We shall ignore this discrepancy between experiment and our model, assigning ω_1 to the stronger, higher-frequency line. For further discussion of the data, we refer the reader to Kahan *et al.*⁶

Knowledge of the 1D potential $v(x)$ is required for further progress. Upon choosing a form for $v(x)$, a Hamiltonian matrix is formed using a harmonic-oscillator basis. The matrix is diagonalized numerically to obtain the eigenvalues and eigenvectors. The parameters of $v(x)$ are varied by a search program to determine the best fit of model frequencies to absorption lines for each strain.

A large variety of double-minimum potentials have been applied to hydrogen bonding, hindered rotation, and other problems. A potential used by Somorjai and Hornig,¹²

$$v(x) = v_4 x^4 + v_2 x^2, \quad (13)$$

seemed particularly suited to our problem. With $v_4 > 0$ and v_2 sufficiently negative, the potential consists of two wells separated by a barrier. When $v_2 > 0$, the potential is a single well. Thus Eq. (13) can account for both on- and off-center behavior. An obvious advantage of this function is that the Hamiltonian matrix is easily computed, since the matrix elements of a polynomial in a harmonic-oscillator basis can be found using creation and destruction operators. The matrix elements are written down by Somorjai and Hornig.¹² The resulting matrix, a band matrix with nonzero elements near the main diagonal only, is preferred for many numerical diagonalization techniques. However, a relatively large number of harmonic-oscillator basis functions is required to obtain accurate values for the eigenvalues. 30×30 matrices were adequate, as we required only the lowest four eigenvalues.

Clayman *et al.*¹³ used a harmonic-oscillator perturbed by a Gaussian barrier,

$$v(x) = Ax^2 + B \exp(-Cx^2), \quad A, B, C > 0 \quad (14)$$

to analyze data on $\text{KBr} : \text{Li}^+$. The term $B \exp(-Cx^2)$ was treated in perturbation theory. For $\text{KCl} : \text{Li}^+$ at low pressures the barrier is too high for perturbation theory to work, so we choose to solve this potential numerically by diagonalizing a 20×20 matrix. A smaller basis of harmonic-oscillator functions gives results comparable to the QH potential calculations because the GB potential is harmonic at large x . A disadvantage of this potential is the need to compute matrix elements for the Gaussian barrier. This difficulty was overcome by using a clever procedure devised by Chan and Stelman¹⁴ that requires calculating only n matrix elements to form an $n \times n$ matrix.

C. Computational methods

The computer calculations were performed on a PDP 11/34 computer. The Hamiltonian matrices were diagonalized using the EISPACK¹⁵ routines TRED2 and TQL2 for real symmetric matrices. Single precision FORTRAN was adequate given the precision of the data.

For the QH model, the potential can be rewritten

$$V(\xi) = \frac{1}{2} \hbar \beta (v_4 \xi^4 + v_2 \xi^2), \quad \xi = (m\beta/\hbar)^{1/2} x, \quad (15)$$

where β is the frequency of the harmonic oscillator defining the basis, m is the mass of a Li^+ impurity, and ξ is x in dimensionless units. β is chosen so that the parameters v_2 and v_4 are of order unity, i.e., the basis harmonic oscillator is selected to roughly overlap the double minimum potential. This choice of basis minimizes the dimension of the Hamiltonian matrix required to achieve the

desired accuracy of the energy eigenvalues. The accuracy of the lowest four eigenvalues of a 30×30 matrix describing $\text{KCl} : \text{Li}^+$ at zero strain was checked by comparison with the results obtained with a 50×50 matrix. The four lowest eigenvalues were in agreement to five significant figures.

The basis set of twenty harmonic-oscillator functions for the GB model was chosen to be eigenfunctions of the oscillator Ax^2 . Again, agreement to five significant figures with the results of calculations using a 50×50 matrix was obtained for the four lowest eigenvalues.

The parameters of the potentials were optimized by the method of parallel tangents, as described in the book by Wilde.¹⁶ The parameters converge quickly when the contours of the function to be optimized are elliptical. In practice, the method worked well when two parameters were adjusted to fit two frequencies. When fits to three transitions were attempted, convergence was slow.

For both models, two parameters were varied to fit assigned frequencies to the appropriate experimental lines. In the QH model v_2 and v_4 were adjustable. The parameters of the GB model were B and C —measures of the magnitude and width of the barrier, respectively. The parameter A specifying the unperturbed harmonic oscillator was fixed in order to reduce the number of variables. The value A was taken from Clayman *et al.*¹³ to match the harmonic part of the potential of $\text{KBr} : \text{Li}^+$ at zero strain. Clayman *et al.* determined A by fitting the energy difference between the ground and first excited states to the observed resonant frequency and its isotope shift. Using this value of A , we were not able to fit absorption spectra, including transitions to the excited-state multiplets, at the highest strains for which data exists for the entire set of lines ($-dr/r \approx 0.8\%$). A larger value of A is required to give a well narrow enough to account for the high-strain data. A narrower well might also improve the fit of the GB model at lower strains, near 0.3%, by pushing the frequency ω_5 up towards the data point (see Fig. 4).

III. RESULTS AND INTERPRETATION

Plots of the QH and GB potentials showing 1D energy levels of $\text{KCl} : \text{Li}^+$ for several values of hydrostatic strain are displayed in Fig. 5. The models are easily distinguished: The GB harmonic envelope is wider than the QH quartic, and the GB barrier is narrower. Note also the monotonic decrease of barrier height with strain.

Figure 4 shows data for the strain dependence of the center frequencies of absorption lines in $\text{KCl} : {}^6\text{Li}^+$ and the corresponding fits for both model

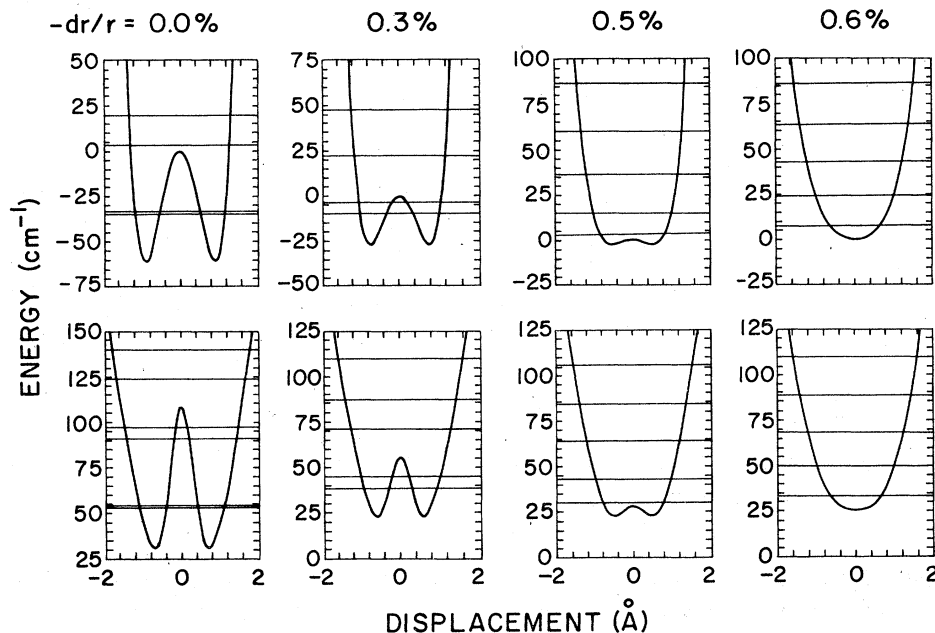


FIG. 5. Model potentials and energy levels for KCl1: ${}^6\text{Li}^+$ at several strains: top row: QH model $v(x) = v_4x^4 + v_2x^2$; bottom row: GB model $v(x) = Ax^2 + B\exp(-Cx^2)$.

potentials. The optimization program attempted to fit the lowest two frequencies, ω_1 and ω_6 , only. For the QH potential we were able to match ω_1 and ω_6 with the data over the entire range of strains shown in the figure.¹⁷ The GB model could not be fit to the data for strains above 0.7% due to the excessive width of the constrained (fixed A) well. The transition ω_4 is completely determined by ω_1 and ω_6 in these models. ω_4 matches the data at low strains, but deviates at large strains. Since ω_4 is electric dipole forbidden in our model, the fact that it is observed at all in addition to the deviation at large strains demonstrates a failure of the separable potential given by Eq. (3) to account precisely for experiment.

The only transition for which the two model potentials give different results is ω_5 . At high strains ($-dr/r > 0.6\%$), for which the potential is a perturbed harmonic oscillator, both models fit the data well. For intermediate strains [$0.3 < -dr/r (\%) < 0.5$] the three-parameter GB model provides a better fit, as the two-parameter QH model misses the data by about 12% of the average of the experimental and theoretical values of ω_5 . However, the fit of ω_5 in the QH model can be improved if we are willing to sacrifice some precision in the fits to ω_1 and/or ω_6 . Given the uncertainty of the experimental determination of ω_6 , as evidenced by the scatter in the data, we conclude that the two-parameter QH potential is able to satisfactorily account for the strain de-

pendence of the four lines shown in Fig. 4. There are no data for ω_5 at strains below 0.25% since the excited-state transitions merge into a single band and cannot be resolved. Absorption frequencies at low strains were obtained by interpolating ω_1 using the zero-strain datum and extrapolating ω_6 from higher strains.

Figure 6 shows the strain dependence of the barrier height V_0 and off-center displacement (coordinate of minimum energy) x_m for both potentials. V_0 is linear up to strains near 0.5%, where the barrier disappears. The linearity is probably a consequence of the approximate linearity in the strain dependence of ω_1 and ω_6 , to which the model potentials were fit. x_m varies linearly with strain up to $-dr/r = 0.4\%$, then falls abruptly to zero. The suddenness of this drop cannot be explained by the idea of two rigid wells pushed together by the application of pressure and remains a puzzle.

On the basis of the plots in Fig. 6, we can identify three regimes of behavior in KCl: Li^+ for strains up to 0.8%:

- (i) The off-center region, $0.0 < -dr/r (\%) < 0.4$, for which the barrier exceeds the ground-state level and tunneling effects are important.
- (ii) The transition region, $0.4 < -dr/r (\%) < 0.6$, where the barrier disappears, but the potential is strongly anharmonic.
- (iii) The perturbed harmonic region, $0.6 < -dr/r (\%) < ?$, where the anharmonicity is a perturbation of decreasing importance relative to the harmonic

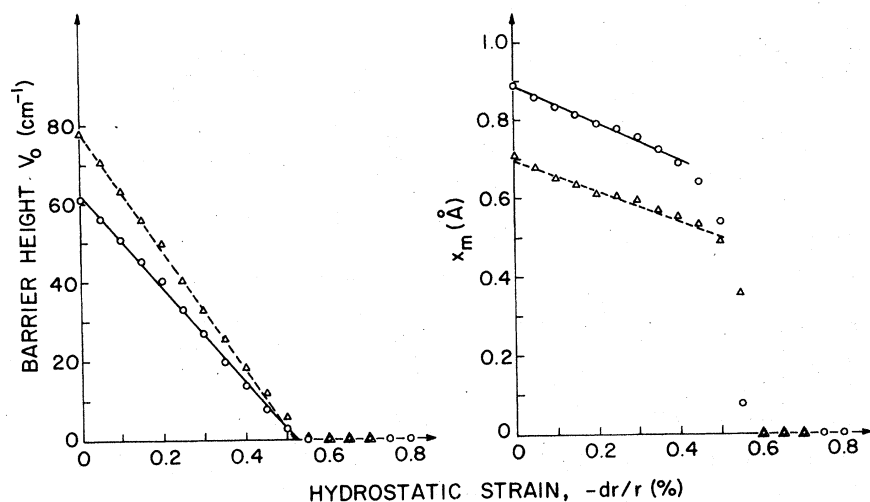


FIG. 6. Strain dependence of model parameters (O, solid line—QH; Δ , dashed line—GB): (a) barrier height V_0 ; (b) off-center displacement of minimum potential energy x_m .

well. A harmonic regime is expected to exist at higher strains. This sectioning closely resembles the partition into regimes suggested by Kahan *et al.*⁶

A remarkable feature of off-center defect systems is the unusually large isotope effect observed

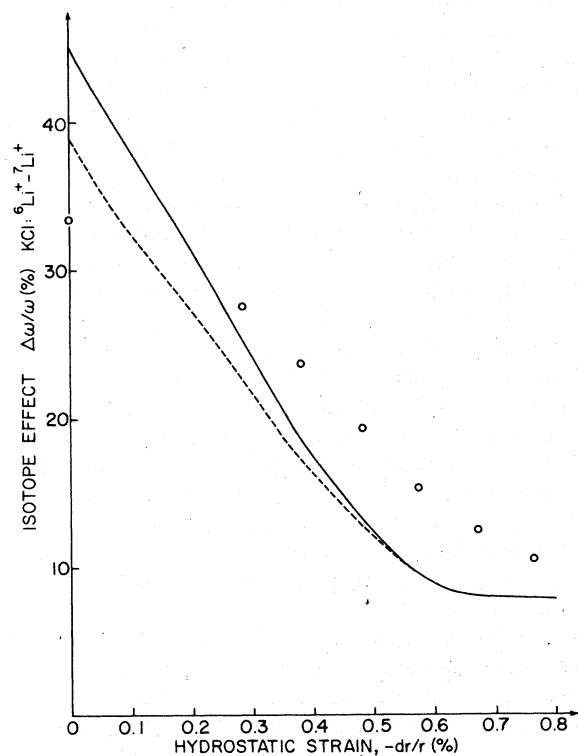


FIG. 7. Strain dependence of $\text{KCl}:\text{}^6\text{Li}-\text{}^7\text{Li}$ isotope effect for transitions within the ground-state multiplet. Circles indicate data, a solid line shows the QH model fit, and the dashed line shows the fit for the GB model.

for transitions within the ground-state multiplet. The strain dependence of the isotope effect in $\text{KCl}:\text{}^6\text{Li}-\text{}^7\text{Li}$ and the fits obtained from our calculations are shown in Fig. 7. Although both fits qualitatively follow the data, the QH fit overshoots the zero-strain isotope effect worse than the GB fit, but gives a better match to the data for intermediate strains. The discrepancy at intermediate strains indicates that our potentials might not be anharmonic enough. Both fits fall off to the harmonic, or Einstein oscillator, limit

$$2(\omega_6 - \omega_7)/(\omega_6 + \omega_7) = 7.7\% \quad (16)$$

(7, 6 denote isotope) more quickly than the data. It is possible to fit both the isotope effect and absorption frequency of the tunneling levels at the expense of missing the excited-state transitions. The inability of the models to fit the complete data exactly might be explained in part as a failure of the form

$$V(x, y, z) = v(x) + v(y) + v(z) \quad (17)$$

but in all likelihood is a manifestation of the failure of the static potential approximation. The approach of the fits to the Einstein oscillator limit at high strains indicates that no effects of the impurity-lattice interaction are built into the potentials at least for high strains. However, the tunneling splitting increases with strain and, since the density of phonons increases as ω^2 (Debye model), if the defect-lattice coupling is significant we expect phonons to play a more important role at high strains. The defect mass enhancement induced by interaction with phonons should remove the asymptotic approach of the tunneling-mode isotope effect to the Einstein limit, so that the isotope effect should continue to drop with increasing strain. Effects of the defect-lattice interaction

TABLE I. Comparison of results.

	$\sqrt{3}x_m^a$ (Å)	$3V_0^b$ (cm ⁻¹)	Dipole moment
			(D)
QH potential	1.55	183	7.44
GB potential	1.23	234	5.91
Quigley and Das	0.44	97	5.15
Experiment	2.54

^a [111] displacement of minimum potential energy.

^b Barrier height for tunneling along body diagonal.

have been discussed in more detail by Page and Helliwell¹⁸ and by Dick.¹⁹

A negative isotope effect has been observed for the 40-cm⁻¹ excited-state absorption band in KCl:Li⁺. Our calculations on static potentials do not exhibit such an effect. However, a possible explanation has been suggested by Benedek.²⁰

Finally, we compare some of our results with the calculations of Quigley and Das^{4,5} (QD). Table I lists the values of $\sqrt{3}x_m$, the displacement of minimum potential in the [111] direction; $3V_0$, the barrier height for tunneling across the main diagonal; and μ , the dipole moment of an off-center ion. We estimate the dipole moment for our potentials using the formula

$$\mu = \sqrt{3}ex_m, \quad (18)$$

where e is the electronic charge. For comparison, the dipole moment measured by Lombardo and Pohl²¹ is also listed. As was the case for the ground-state multiplet (tunneling-mode) isotope effect and the frequencies ω_4 and ω_5 , we did not attempt to fit the dipole moment when we varied the parameters of the model potentials. However, the two-parameter QH potential is still able to give a dipole moment within a factor of three of experiment, and the GB prediction is not much worse than the results of the elaborate QD calculation. The QH and GB potentials exhibit larger off-center displacements and barrier heights than the results of QD. The large central barrier is an attribute of the general form given by Eq. (17), but the large values of $\sqrt{3}x_m$ must arise from fitting transitions involving excited-state multiplets as well as transitions within the tunneling multiplet. These results might be another indication of the importance of the defect-lattice interaction in determining the frequencies of the excited-state absorption band, since the small displacements obtained by QD arise from detailed calculations taking all static forces into account.

IV. SUMMARY

We have performed model calculations on a separable static 3D potential to gain insight regarding the strain-dependent far-infrared properties of KCl:Li⁺. Two 1D model potentials, a quartic well with a quadratic bump (QH) and a harmonic well perturbed by a Gaussian barrier (GB), were fitted to the data of Kahan *et al.*⁶ Both models were able to match the strain-dependent absorption spectrum of KCl:Li⁺, but the QH potential has the advantage of one less parameter. The fits to the isotope effect for transitions within the ground-state multiplet were not so precise. This discrepancy between the models and experiment was suggested to arise from further anharmonicities in the impurity potential and interaction of the localized defect modes with the host lattice. Examination of the strain dependence of the parameters V_0 and x_m revealed surprisingly simple behavior. V_0 was linear in strain up to the point at which the barrier vanished. x_m was weakly linear in strain, but abruptly dropped to zero as the barrier disappeared. The physics underlying this behavior remains unexplained. We suggest that the data can be divided into three regions of behavior for $0.0 < -\dot{x}r/r(\%) < 0.6$: off-center (tunneling) behavior, a very anharmonic transition region, and a perturbed harmonic region. We conclude that the potential

$$V(x, y, z) = v(x) + v(y) + v(z), \quad (19)$$

where $v(x)$ is a symmetric double minimum potential of the QH type is a good first approximation to explaining the properties of low-frequency defect modes in KCl:Li⁺, but that some of the puzzles uncovered by this work remain as topics for future investigations.

ACKNOWLEDGMENTS

We wish to thank R. Aurbach, C. W. Liew, and E. A. Schiff for valuable discussion and assistance. One of the authors (R.P.D.) was supported during this work by a NSF graduate fellowship. This work has been supported in part by the Department of Energy under Contract No. EG-77-S-03-1456. Support has also been received from the Materials Science Center at Cornell University.

- ¹Two recent reviews are A. S. Barker, Jr., and A. J. Sievers, *Rev. Mod. Phys.* **47**, S1-179 (1975); and F. Bridges, *CRC Crit. Rev. Solid State Sci.* **5**, 1 (1975).
- ²I. G. Nolt and A. J. Sievers, *Phys. Rev.* **174**, 1004 (1968).
- ³W. D. Wilson, R. D. Hatcher, G. J. Dienes, and R. Smoluchowski, *Phys. Rev.* **161**, 888 (1967).
- ⁴R. J. Quigley and T. P. Das, *Phys. Rev.* **164**, 1185 (1967).
- ⁵R. J. Quigley and T. P. Das, *Phys. Rev.* **177**, 1340 (1969).
- ⁶A. M. Kahan, M. Patterson, and A. J. Sievers, *Phys. Rev. B* **14**, 5422 (1976).
- ⁷M. Gomez, S. P. Bowen, and J. A. Krumhansl, *Phys. Rev.* **153**, 1009 (1967).
- ⁸These transitions were erroneously labeled electric dipole allowed by Kahan *et al.* (Ref. 6.).
- ⁹J. P. Harrison, P. P. Peressini, and R. O. Pohl, *Phys. Rev.* **171**, 1037 (1968).
- ¹⁰R. D. Kirby, A. E. Hughes, and A. J. Sievers, *Phys. Rev. B* **2**, 481 (1970).
- ¹¹M. C. Hetzler, Jr. and D. Walton, *Phys. Rev. B* **8**, 4801 (1973).
- ¹²R. L. Somorjai and D. F. Hornig, *J. Chem. Phys.* **36**, 1980 (1962).
- ¹³B. P. Clayman, R. D. Kirby, and A. J. Sievers, *Phys. Rev. B* **3**, 1351 (1971).
- ¹⁴S. I. Chan and D. Stelman, *J. Chem. Phys.* **39**, 545 (1963).
- ¹⁵B. T. Smith, J. M. Boyle, B. S. Garbow, Y. Ikebe, V. C. Klema, and C. B. Moler, *Matrix Eigensystem Routines—EISPACK Guide* (Springer-Verlag, Berlin, 1974).
- ¹⁶D. J. Wilde, *Optimum Seeking Methods* (Prentice-Hall, Englewood Cliffs, N. J., 1964).
- ¹⁷The fits were actually made to points evenly spaced in strain (at 0.05% intervals) obtained by interpolating the data. In the case of ω_6 , the models were fit to a smooth curve neglecting the scatter in the data.
- ¹⁸J. B. Page, Jr. and K. G. Helliwell, *Phys. Rev. B* **12**, 718 (1975); J. B. Page, Jr. *Phys. Rev. B* **10**, 719 (1974).
- ¹⁹B. G. Dick, *Phys. Rev. B* **16**, 3359 (1977).
- ²⁰G. Benedek, *Phys. Status Solidi* **43**, 509 (1971).
- ²¹G. Lombardo and R. O. Pohl, *Phys. Rev. Lett.* **15**, 291 (1965).